

RESEARCH ARTICLE

10.1002/2015TC003880

Key Points:

- GPS measurements reveal a sharp velocity gradient zone in eastern Tibet
- The Longriba fault zone is the key structure responsible for this gradient zone
- The Longriba tectonic boundary marks the westernmost edge of the Yangtze block

Correspondence to:

R. Gao,
ruigao126@126.com

Citation:

Guo, X., R. Gao, X. Xu, G. R. Keller, A. Yin, and X. Xiong (2015), Longriba fault zone in eastern Tibet: An important tectonic boundary marking the westernmost edge of the Yangtze block, *Tectonics*, 34, 970–985, doi:10.1002/2015TC003880.

Received 10 MAR 2015

Accepted 14 APR 2015

Accepted article online 21 APR 2015

Published online 16 MAY 2015

©2015. The Authors.

This is an open access article under the terms of the Creative Commons Attribution-NonCommercial-NoDerivs License, which permits use and distribution in any medium, provided the original work is properly cited, the use is non-commercial and no modifications or adaptations are made.

Longriba fault zone in eastern Tibet: An important tectonic boundary marking the westernmost edge of the Yangtze block

Xiaoyu Guo^{1,2}, Rui Gao¹, Xiao Xu³, G. Randy Keller², An Yin⁴, and Xiaosong Xiong¹

¹State Key Laboratory of Continental Tectonics and Dynamics, Key Laboratory of Earthprobe and Geodynamics, MLR, Institute of Geology, Chinese Academy of Geological Sciences, Beijing, China, ²School of Geology and Geophysics, University of Oklahoma, Norman, Oklahoma, USA, ³Chinese Academy of Geological Sciences, Beijing, China, ⁴Department of Earth and Space Sciences, University of California, Los Angeles, California, USA

Abstract Global Positioning System (GPS) measurements across eastern Tibet reveal a sharp velocity gradient zone located about 150 km west of the Longmen Shan frontal thrust zone, where eastward block motion of Tibet decreases from ~12 mm/yr to ~3 mm/yr over a distance of less than 10 km. In order to investigate the tectonic cause for this rapid change in GPS velocity, together with systematic review on the available geological and geophysical data in easternmost Tibet, we provide new constraints on the tectonic feature of the Longriba fault zone from Advanced Land Observing Satellite Phased Array type L-band Synthetic Aperture Radar data. We propose that the NE striking Longriba fault zone is the key structure responsible for the observed sharp gradient in GPS velocities. In addition, the evidence indicates that the Longriba fault zone, instead of the Longmen Shan fault zone, marks the westernmost edge of the Yangtze crustal block. Given the irregular western margin of the Yangtze block, the Longriba fault zone represents part of the actual tectonic boundary between the Songpan-Ganzi terrane and the Yangtze block. The newly identified western edge of the Yangtze block implies a paleocontinent-ocean boundary at depth. This boundary was a potential weak zone and may have been exploited during the formation of the Longriba fault zone. The results of this paper should advance our understanding of the tectonic relationship between the Songpan-Ganzi terrane and Yangtze block and provide additional constraints for studies of the geodynamic response of eastern Tibet to the ongoing India-Eurasia collision.

1. Introduction

The Songpan-Ganzi terrane occupies a large part of the northeastern Tibetan Plateau between the East Kunlun fault on the north and the Qiangtang terrane in the south (Figure 1). It is characterized by the extensive exposure of intensely folded Triassic flysch sequences [e.g., Yin and Harrison, 2000]. The Tibetan Plateau itself is undergoing eastward block motion as a response to the ongoing India-Eurasia collision [e.g., Burchfiel et al., 1995; Tapponnier et al., 2001]. Across eastern Tibet, Global Positioning System (GPS) measurements reveal a decrease of the eastward velocities by 10–15 mm/yr when approaching the Longmen Shan fault zone and western Sichuan basin [Taylor and Yin, 2009]. In addition, in the region located ~150 km northwest of the Longmen Shan fault zone, GPS measurements detect a remarkable velocity gradient along an unmapped shear zone situated subparallel to the Longmen Shan fault zone [Lv et al., 2003; Shen et al., 2005], where the eastward block motion of Tibet decreases from ~12 mm/yr to ~3 mm/yr over a distance of no more than 10 km [King et al., 1997; Chen et al., 2000; Lv et al., 2003; Shen et al., 2005]. This velocity gradient zone was named the “Ma’erkang velocity gradient zone” [Lv et al., 2003] or “Songpan-Xihe deformation zone” [Shen et al., 2005], and active crustal shortening was proposed to be accommodated along this zone [Taylor and Yin, 2009].

This discovery was puzzling until 2008 when field investigations of the geometry of this velocity gradient recognized that it correlates with an active zone of faulting, the Longriba fault zone [Xu et al., 2008; Ren et al., 2013a, 2013b]. This fault zone consists of the dextral transpressive Longriq fault to the northwest and the pure right-lateral Mao’ergai fault to the southeast [Xu et al., 2008; Ren et al., 2013a, 2013b]. These two subparallel faults have a length of more than 100 km each and are spaced about 30 km apart. Large-scale intracontinental strike-slip faults are generally located adjacent to regions with contrasting physical properties [Molnar and Dayem, 2010]. Thus, as a newly discovered intracontinental strike-slip fault zone,

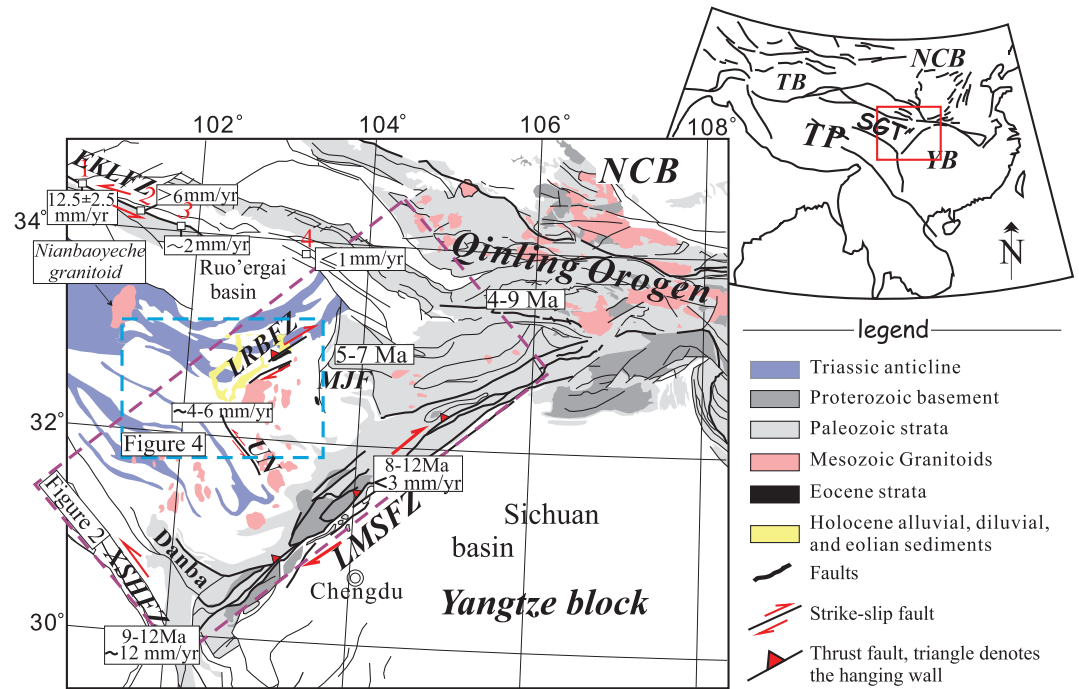


Figure 1. Generalized geological map of the eastern Tibetan Plateau (based on the 1:2.5 million scale geological map of China); inset figure shows the location of research area. Numbers 1, 2, 3, and 4 in red indicate the four sites where Kirby *et al.* [2007] obtained the slip rate of the eastern segment of the Kunlun fault zone. The slip rate of each major fault is from Chen *et al.* [2000] and Kirby *et al.* [2007]. Please refer to text for references of onset of deformation of each tectonic unit. The purple dashed box in the main figure shows the geographic location of Figure 2. The blue dashed box shows the geographic location of Figure 4. NCB = north China block, YB = Yangtze block, TP = Tibetan Plateau, TB = Tarim basin, KF = Kunlun fault, LMSfZ = Longmen Shan fault zone, LRBfZ = Longriba fault zone, EKLfZ = eastern Kunlun fault zone, XSHF = Xianshuihe fault, and UN = unnamed fault.

the Longriba fault zone has attracted considerable interest [e.g., Lv *et al.*, 2003; Shen *et al.*, 2005; Xu *et al.*, 2008; Ren *et al.*, 2013a, 2013b]. However, the tectonic driver for the Longriba fault zone remains ambiguous, although it has been considered a high-risk zone for large earthquakes [Ren *et al.*, 2013b]. It has been proposed that initiation of the Longriba fault zone is due to the accommodation of a differential block movement from the western Songpan-Ganzi terrane toward the east [Xu *et al.*, 2008]. However, the question of what would cause such a movement within the interior of the Songpan-Ganzi terrane is not addressed, which is in turn a vital key to understanding the tectonics of this intracontinental strike-slip fault zone. In addition, an unnamed (UN) fault subperpendicular to the Longriba fault zone to the southwest (Figures 1 and 6) shows an obvious Coulomb stress change with a sinistral sense of movement [Nalbant and McCloskey, 2011], which makes the initiation of the Longriba fault zone enigmatic.

Thus, to fully understand the tectonic history of the Longriba fault zone, a first thorough understanding of the regional tectonic characteristics of the Songpan-Ganzi terrane is needed. In this paper, we review and summarize the previous studies regarding the tectonic and magmatic history of the Songpan-Ganzi terrane. Past tectonic events may have provided geological conditions for the initiation of the Longriba fault zone, and therefore, its tectonic setting will be discussed. Our goals are to advance the understanding of the tectonic interactions between the Songpan-Ganzi terrane and Yangtze block since the early Mesozoic and to provide constraints on the tectonic response of the eastern Tibetan Plateau to the ongoing India-Eurasia collision.

2. Geological Background of Eastern Tibet

As one of the tectonic elements of the Tibetan Plateau, the Songpan-Ganzi terrane in northeastern Tibet is dominantly featured with a widespread Triassic flysch complex, as well as Mesozoic volcanism and diachronous thrusting events (Figure 1). Given the complex tectonic history of this region, the sequence of

geological events prior to the India-Eurasia collision may exert a strong influence on the Cenozoic structural configuration and crustal composition.

2.1. Mesozoic Tectonic History

The Songpan-Ganzi terrane has experienced multiple tectonic events since the early Mesozoic. The nature of the Songpan-Ganzi terrane basement, however, remains unknown, as it has been hidden below the allochthonous Triassic flysch wedge, which is 5–15 km thick and covers a triangular area over 200,000 km² [Huang and Chen, 1987; Nie *et al.*, 1994; Zhou and Graham, 1996; Chang, 2000] (Figure 1). Although there is considerable debate about the detrital provenance of the turbidite sources of the Songpan-Ganzi terrane [e.g., Nie *et al.*, 1994; Avigad, 1995; Zhou and Graham, 1996; Chang, 2000; Weislogel *et al.*, 2006; Enkelmann *et al.*, 2007; Burchfiel and Chen, 2012], most hypotheses favor the concept that the turbidites were deposited in a remnant ocean, which developed after the Paleo-Tethys Ocean was consumed as a result of interactions between the north China, south China, and Qiangtang blocks [e.g., Chang, 2000; Yin and Nie, 1993; Nie *et al.*, 1994; Pullen *et al.*, 2008]. Diachronous magmatism and orogenic events contemporaneously occurred around the Songpan-Ganzi Remnant Ocean, including the collision between the south China and north China blocks in the Early Triassic [Chang, 2000; Yin and Nie, 1993; Nie *et al.*, 1994; Guo *et al.*, 2012], as well as subduction of the Paleo-Tethys along the Kunlun fault zone to the north and oceanic subduction along the Ganzi-Litang suture zone to the south [Reid *et al.*, 2005, 2007; Roger *et al.*, 2011].

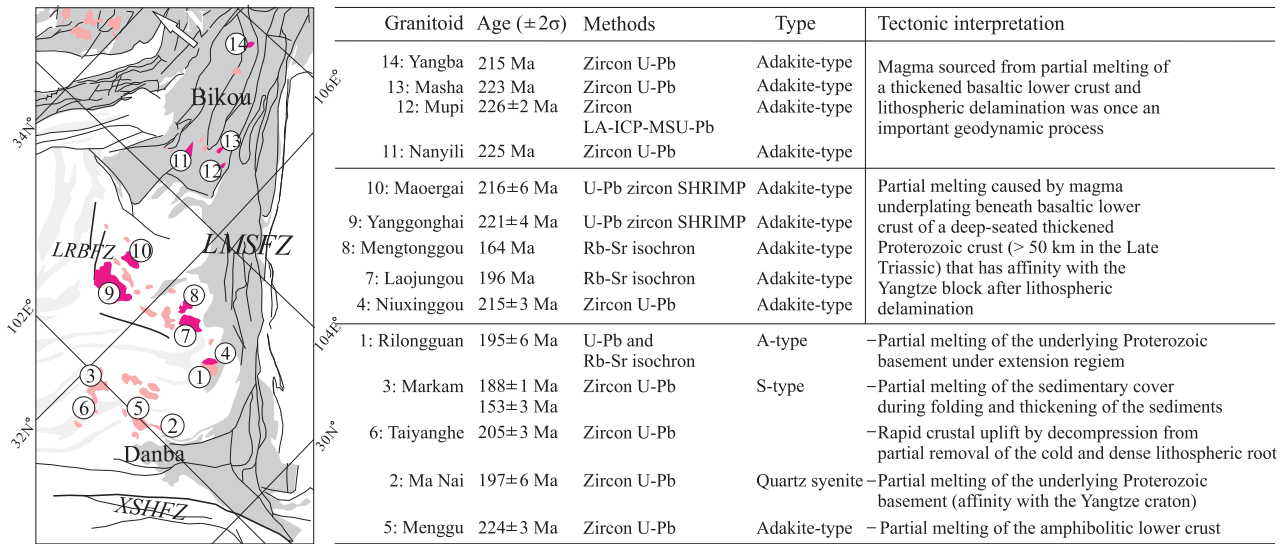
There was the Yangtze block (northern part of the south China block) to the east of the Songpan-Ganzi Remnant Ocean, where the passive margin of the Yangtze block was juxtaposed with the remnant ocean [e.g., Roger *et al.*, 2004; Harrowfield and Wilson, 2005; Zhang *et al.*, 2006] and the Triassic flysch sediment progressively overlapped the western passive margin of the Yangtze block [Harrowfield and Wilson, 2005]. During the Indosinian orogeny (Late Paleozoic-Early Mesozoic), coeval subduction occurred in the north and southwest of the Songpan-Ganzi Remnant Ocean [e.g., Reid *et al.*, 2005, 2007; Roger *et al.*, 2011]. As a result of northeast-southwestward crustal shortening and subsequent southeast directed thrusting toward the western passive margin of the Yangtze block [Roger *et al.*, 2004, 2010], the Songpan-Ganzi Remnant Ocean and its sedimentary fill experienced intense deformation; flysch units were shortened and folded along a series of northwest-southeast trending anticlines (Figure 1). Additionally, the sinistral transpressive Longmen Shan (LMS) thrust-nappe belt (Figure 1) was initiated as a convergent zone between the Songpan-Ganzi terrane and Yangtze block [Burchfiel *et al.*, 1995]. Upright axial planes of the anticlines are perpendicular to the LMS fault zone in the south but change to parallel the LMS fault zone in the north (Figure 1). In addition, Triassic lithospheric delamination occurred beneath the Songpan-Ganzi Remnant Ocean [Zhang *et al.*, 2006, 2007a, 2007b]. As a result, Triassic syntectonic to late tectonic granitoids (220–200 Ma), as well as postorogenic granitoids (200–150 Ma), are widely distributed in the Songpan-Ganzi terrane [e.g., Roger *et al.*, 2004; Zhang *et al.*, 2006] (Figure 1).

The eastern Songpan-Ganzi terrane experienced slow cooling ($\sim 3^\circ\text{C}/\text{Myr}$) during Late Mesozoic between the Late Jurassic to early Cenozoic [Roger *et al.*, 2011], indicating a lack of major tectonic events after the amalgamation of the Songpan-Ganzi terrane and Yangtze block in the early Cenozoic [Burchfiel *et al.*, 1995; Roger *et al.*, 2011]. Little direct evidence of tectonic activity has been observed except the continued westward deposition of conglomerates of this age along the foredeep of the Longmen Shan [Burchfiel *et al.*, 1995; Meng *et al.*, 2005]. Cenozoic shortening across the Longmen Shan range was minor [Burchfiel *et al.*, 1995].

2.2. Cenozoic Tectonic History

During the Cenozoic, the eastern Tibetan Plateau has been very tectonically active and is currently undergoing eastward block motion as a response to the collision between India and Eurasia [e.g., Dewey *et al.*, 1988; Yin and Harrison, 2000; Yin, 2010a]. As a result, eastern Tibet experienced a rapid increase in mean elevation beginning in the late Miocene [Clark *et al.*, 2005].

In the southeastern Tibetan Plateau, the onset of rapid cooling that initiated along the sinistral strike-slip Xianshuihe fault zone has been constrained to be around 9–12 Ma [Clark *et al.*, 2005]. The continuous slip rate observed is 12 ± 2 mm/yr [Chen *et al.*, 2000] (Figure 1). Two pulses of accelerated exhumation in the Longmen Shan range have been inferred to have begun at 8–12 Ma and 7–5 Ma (late Miocene) [Arne *et al.*, 1997; Kirby *et al.*, 2002; Enkelmann *et al.*, 2006; Kirby, 2008; Ouimet *et al.*, 2010; Wilson and Fowler, 2011;



Refs: (1-3): Roger et al. 2004; (4-6):Yuan et al., 2010; (7-8): Yuan et al., 1991, Yuan and Zhang, 1994, Zhao et al., 2007; (9-10): Zhang et al., 2006; (11): Zhang et al., 2007a; (12): Zhang et al., 2007a, Lu et al., 2010; (13): Lu et al., 2010; (14): Zhang et al., 2007a

Figure 2. Synthesis of the available geochemical and geochronological constraints on the Early Mesozoic granitoids in eastern Tibet and related tectonic implications; granitoids in bright purple indicate that the adakite-type granitoids have affinity with the Yangtze basement. The granitoids are numbered according to the sequence they appear in the text.

Wang et al., 2012]. However, no significant eastward convergence (<3 mm/yr) between eastern Tibet and the Sichuan basin has been observed [Shen et al., 2005, 2009; Gan et al., 2007].

Along the Kunlun fault that is the northern boundary of the Songpan-Ganzi terrane (Figure 1), initial sinistral shear along the fault zone during Cenozoic is poorly understood, although initiation of sinistral shearing in the westernmost portion of this fault zone has been inferred to be coeval with the Miocene (~15 Ma) expansion of the Tibetan Plateau [Jolivet et al., 2003]. The slip rate of the eastern Kunlun fault decreases systematically toward the east from around Dawu at 12.5 ± 2.5 mm/yr (site 1), through the Ken Mu Da at <6 mm/yr (sites 2 and 3) to ≤ 1 mm/yr along the Tazang fault zone (site 4) [Kirby et al., 2007] (Figure 2). In the northeastern Tibetan Plateau, the western Qinling orogen that was affected by the rising plateau experienced rapid cooling at 9–4 Ma, which is constrained by apatite fission track thermochronology data to be a few million years later than in eastern Tibet [Enkelmann et al., 2006].

In the interior of the Songpan-Ganzi terrane, the Longriba fault zone that was first recognized by Xu et al. [2008] is located in another area where rapid changes in lateral rates of movement occur [Lv et al., 2003; Shen et al., 2005] (Figure 1). Xu et al. [2008] suggested that the Longriba fault zone is an active late Quaternary feature, but precise timing of its initiation is lacking. The Longriba fault zone consists of two parallel faults (Longriqu and Mao’ergai faults) that have experienced different slip rates. According to Xu et al. [2008], the Longriqu fault has experienced 3.7 ± 0.3 mm/a dextral shearing rate and 0.7 mm/a vertical slip rate since the late Quaternary, and the Mao’ergai fault has a 3.6 ± 0.5 mm/a dextral strike-slip rate. A combined study of field investigations and radiocarbon and optically stimulated luminescence dating by Ren et al. [2013a] indicates that the slip rate along the Longriba fault zone has decreased from ~7.5 mm/yr in the latest Pleistocene to ~2.1 mm/yr in the Holocene.

Additionally, as a result of the ongoing convergence between India and Eurasia, the northeastern to eastern margin areas of Tibet have been seismically active. Several large earthquakes have been recorded, such as the 1933 M_w 7.5 Diexi earthquake and the 1976 M_w 7.2, 6.7, and 7.2 Songpan earthquake swarm around the Min Shan area of the northeastern Songpan-Ganzi terrane [e.g., Chen et al., 1994], as well as the 2008 M_w 7.9 Wenchuan earthquake and the 2013 M_w 7.0 Ya’an earthquake of the eastern margin of Tibet [e.g., Yin, 2010b; Guo et al., 2014]. However, the Longmen Shan range had been seismically quiescent before 2008, and no earthquakes of $M_w \geq 7.0$ had been historically reported. The Longriba fault zone of the interior of the Songpan-Ganzi terrane has no historical record of significant earthquake activity, but

paleoseismic studies have revealed that a sequence of earthquakes of magnitude >7.0 occurred along it [Ren *et al.*, 2013b], and this fault zone viewed as having a high potential for large earthquakes in the near future [Ren *et al.*, 2013b].

2.3. Granitoid Constraints on the Nature of the Basement

Granitoids are the one of the most common rocks in the Earth's crust. However, information that can be gained from them is significant, as (a) their isotopic compositions can be matched with isotopically unique crust and therefore provide constraints on their crustal source [e.g., Maniar and Piccoli, 1989]; (b) their ages provide direct evidence for the timing of magmatism, which might be linked to tectonic events, such as delamination [e.g., Sun *et al.*, 2002]; and (c) their major and trace element composition (adakitic, for example) may be used to infer crustal thickness (at least 50 km) and type of source rock (eclogitic or garnet amphibolite) [e.g., Hacker, 1996]. Specifically, adakitic granitoids are sourced from andesitic-dacitic (diorite-tonalite) magmas with evidence that is consistent with their formation by melting of basaltic source rocks in the eclogite or garnet amphibolites facies (i.e., depths of about 50 km or greater) [Hacker, 1996; Zhang *et al.*, 2006]. As such, their presence and ages may provide evidence for the timing of the formation of thickened crust with basaltic roots.

In the eastern Songpan-Ganzi terrane, granitoids are widespread and cut through the Triassic fold belts, showing sharp contacts with them (Figures 1 and 2). In the southeastern Songpan-Ganzi terrane (Figure 2), Roger *et al.* [2004] separated the granitoids into amphibole granites (197 ± 6 Ma, U-Pb zircon) in the Rilongguan (1 in Figure 2) and Ma Nai (2 in Figure 2) areas and biotite and/or muscovite granites (188 ± 2 Ma and 153 ± 2 Ma, U-Pb zircon) in the Markam area (3 in Figure 2). Partial melting of the underlying basement (south China or Songpan-Ganzi terrane Proterozoic basement) probably provided sources for the Rilongguan and Ma Nai granites [Roger *et al.*, 2004]. The Rilongguan plutons are A-type granites (1 in Figure 2), and the Ma Nai granites (2 in Figure 2) belong to the quartz syenite group [Roger *et al.*, 2004]. However, the Markam (Ke'eryin) granites (3 in Figure 2) might have resulted from partial melting of Middle Triassic sediments and have been categorized as S-type granite [Roger *et al.*, 2004].

Yuan *et al.* [2010] further separated the Niuxinggou granites (4 in Figure 2) from the northern Rilongguan granites and carried out detailed geochemical studies. Their research results indicate that the Niuxinggou granites are adakite-type granites and yield a 215 ± 3 Ma crystallization age. Thus, formation of the Niuxinggou granites was much older than that of the Rilongguan granites, and different partial melting sources were identified [Roger *et al.*, 2004; Yuan *et al.*, 2010]. The other two granitic plutons studied by Yuan *et al.* [2010] were the Menggu granites (5 in Figure 2) and the Taiyanghe granites (6 in Figure 2). Yuan *et al.* [2010] found that the Menggu granite (224 ± 3 Ma) was sourced from partial melting of amphibolitic lower crust and was categorized as an adakite-type granite. The Taiyanghe granites yielded a crystallization age of 205 ± 3 Ma and were sourced from low degrees of partial melting of a metasomatized lithospheric mantle [Yuan *et al.*, 2010]. Both the Menggu pluton and the Niuxinggou pluton are related to crustal thickening [Yuan *et al.*, 2010]. Formation of the Taiyanghe granitoid was, however, related to rapid crustal uplift during partial removal of the cold and dense lithospheric root [Yuan *et al.*, 2010].

In the northeastern portion of the eastern Songpan-Ganzi terrane and the Bikou terrain (Figure 2), a more uniform granitic type is found relative to those in the southwestern area of the eastern Songpan-Ganzi terrane discussed above, which mostly falls in the adakite-type granite category [e.g., Zhang *et al.*, 2006, 2007a; Li *et al.*, 2007; Zhao *et al.*, 2007; Lu *et al.*, 2010]. Among these granitoids, the Laojunggou (7 in Figure 2) and Mentonggou (8 in Figure 2) plutons yield 196 Ma and 164 Ma Rb-Sr isochron ages, respectively [Yuan *et al.*, 1991; Yuan and Zhang, 1994]. Geochemical analyses of these plutons indicate that they possess crustal Nd-Sr isotope compositions, and therefore, they mostly likely resulted from partial melting of the lower crustal instead of mantle-derived materials [Zhao *et al.*, 2007]. The Yanggonhai (9 in Figure 2) and Maoergai (10 in Figure 2) granitoids in the east central Songpan-Ganzi terrane yield 221 ± 3.8 Ma and 216 ± 5.7 Ma magma crystallization ages, respectively [Zhang *et al.*, 2006]. Geochemical signatures of these two granitoids indicate adakite-type formation [Zhang *et al.*, 2006]. Four granitoids were identified with adakitic geochemical signatures in the Bikou terrain (Figure 2), which are the Nanyili granitoid (11 in Figure 2) [Zhang *et al.*, 2007a], Mupi granitoid (12 in Figure 2) [Zhang *et al.*, 2007a; Lu *et al.*, 2010], Mashan granitoid (13 in Figure 2) [Lu *et al.*, 2010], and Yangba granitoid (14 in Figure 2) [Zhang *et al.*, 2007a]. Crystallization ages of the Nanyili and Yangba granitoids are 215 Ma and 225 Ma, respectively [Zhang *et al.*, 2007a]. Zircon laser ablation-inductively

Table 1. Information on Available Seismic Experiments in the Eastern Tibetan Plateau

| No. | Profile Name | Observing Year | Length | Reference |
|-----|--|----------------|-------------|---|
| ① | Zhubalong-Zizhong | 2000 | 552 km | <i>Wang et al.</i> [2003a] |
| ② | Beizilan-Tangke | 2000 | 649.1 km | <i>Wang et al.</i> [2003b] |
| ③ | Longmen Shan triangle | 1979–1983 | three shots | <i>Chen et al.</i> [1988] |
| ④ | GGT Altai-Taiwan (Altyn Tagh-Longmen Shan) | 1987 1989 | 1600 km | <i>Wang et al.</i> [2005] |
| ⑤ | GGT Altai-Taiwan (Heishui-Shaoyang) | 1986 | 2200 km | <i>Cui et al.</i> [1996] |
| ⑥ | Ma'erkang-Gulang SinoProbe-02 | 2004 | 637 km | <i>Zhang et al.</i> [2008] |
| ⑦ | SinoProbe-02 refraction profile | 2011 | 410 km | X. Xu et al. (Uplift of the Longmen Shan Area in the Eastern Tibetan Plateau: An integrated geophysical and geodynamic analysis, submitted to <i>International Geology Review</i> , 2015) |
| ⑧ | Ruo'ergai deep reflection profile | 2007 | 115 km | <i>Wang et al.</i> [2011] |
| ⑨ | SinoProbe-02 deep reflection profile | 2011 | 312 km | <i>Guo et al.</i> [2013, 2014] |

coupled plasma–mass spectrometry–Pb analysis of the Mupi granitoid yielded a 226 ± 2 Ma crystallization age [Lu et al., 2010]. Similarly, geochemical signatures of these adakite-type granitoids indicate that the related magma sources resulted from partial melting of the thickened basaltic lower crust of an unexposed continent-type basement beneath the Bikou Group volcanic rocks [Zhang et al., 2007a; Lu et al., 2010].

Pb-Sr-Nd isotopic compositions of these adakite-type granitoids reveal the existence of deeply buried, thickened Proterozoic basement that has affinity with the Yangtze block beneath the eastern Songpan-Ganzi terrane [e.g., Zhang et al., 2006, 2007a]. Although adakite is not the only magma type that can be produced from the lower part of thickened crust, it is notable that the adakitic granitoids are clustered in the NE, where other lines of evidence suggest the existence of thickened continental crust to over 50 km after lithospheric delamination [Burchfiel et al., 1995; Yin and Harrison, 2000; Guo et al., 2013].

2.4. Crustal Structure of Eastern Tibet

Since the 1980s, substantial efforts have been made in exploring the crustal structure of the eastern Tibetan Plateau and adjacent areas (Table 1). These efforts include passive source tomography and receiver function studies, as well as active source seismic refraction/wide-angle reflection and deep reflection profiling experiments [e.g., Chen et al., 1988; Wang et al., 2003a, 2003b; Wang et al., 2004, 2005; Gao et al., 2005; Li et al., 2006; Wang et al., 2007; Wang et al., 2011; Zhang et al., 2008; Liu et al., 2008; Zhang et al., 2010; Guo et al., 2013, 2014]. The location of each experiment in our study area is shown in Figure 4. The detailed information about the seismic experiments in the eastern Tibetan Plateau can be found in Table 1.

Previous seismic refraction studies indicate that the depth of the crustal mantle boundary (Moho) varies significantly beneath the eastern Tibetan Plateau [Chen et al., 1988; Li et al., 2006; Zhang et al., 2008]. Wang et al. [2003a] conducted a teleseismic receiver function analysis along an E-W profile that approximately follows 30°N and indicates a Moho step from 42.9 km beneath the Sichuan basin to 59.8–63 km beneath the southeastern Songpan-Ganzi terrane (line 1; Figure 3). It is consistent with the studies by Zhang et al. [2009] and Wang et al. [2010] that there is a rapid change of Moho depth across the LMS fault zone from ~42 km at the range front to ~60 km west of the range. In addition, the NNE trending receiver function profile of Wang et al. [2003b] (line 2; Figure 6) shows that there is a gradual southward increase in crustal thickness from ~50 km in the north. The crustal thickness is variable along the LMS fault zone as well, deepening from ~43.2 km beneath the northeastern segment to ~48.3 km beneath the southwestern segment [Wang et al., 2010]. Thus, crustal thickness of the eastern Tibetan Plateau decreases toward the northeast behind the LMS range but shows a local increase when approaching the LMS range.

Variations of crustal thickness beneath the eastern Tibetan Plateau have been constrained by several seismic refraction studies [e.g., Wang et al., 2003a; Li et al., 2006; Zhang et al., 2008], and previous seismic refraction studies provided detailed information about the crustal structure. So far, two seismic reflection experiments have been conducted in eastern Tibet, which are the Ruo'ergai seismic reflection experiment [Wang et al., 2011] (line 8; Figure 3) and the 2011 SinoProbe-02 Longmen Shan seismic reflection experiment [Guo et al., 2013, 2014] (line 9; Figure 3). One of the most important contributions of these two seismic reflection profiles is to have documented the existence of the Yangtze crystalline crust beneath the easternmost Tibetan Plateau, which has been highly thrust and shortened to thickness over 50 km.

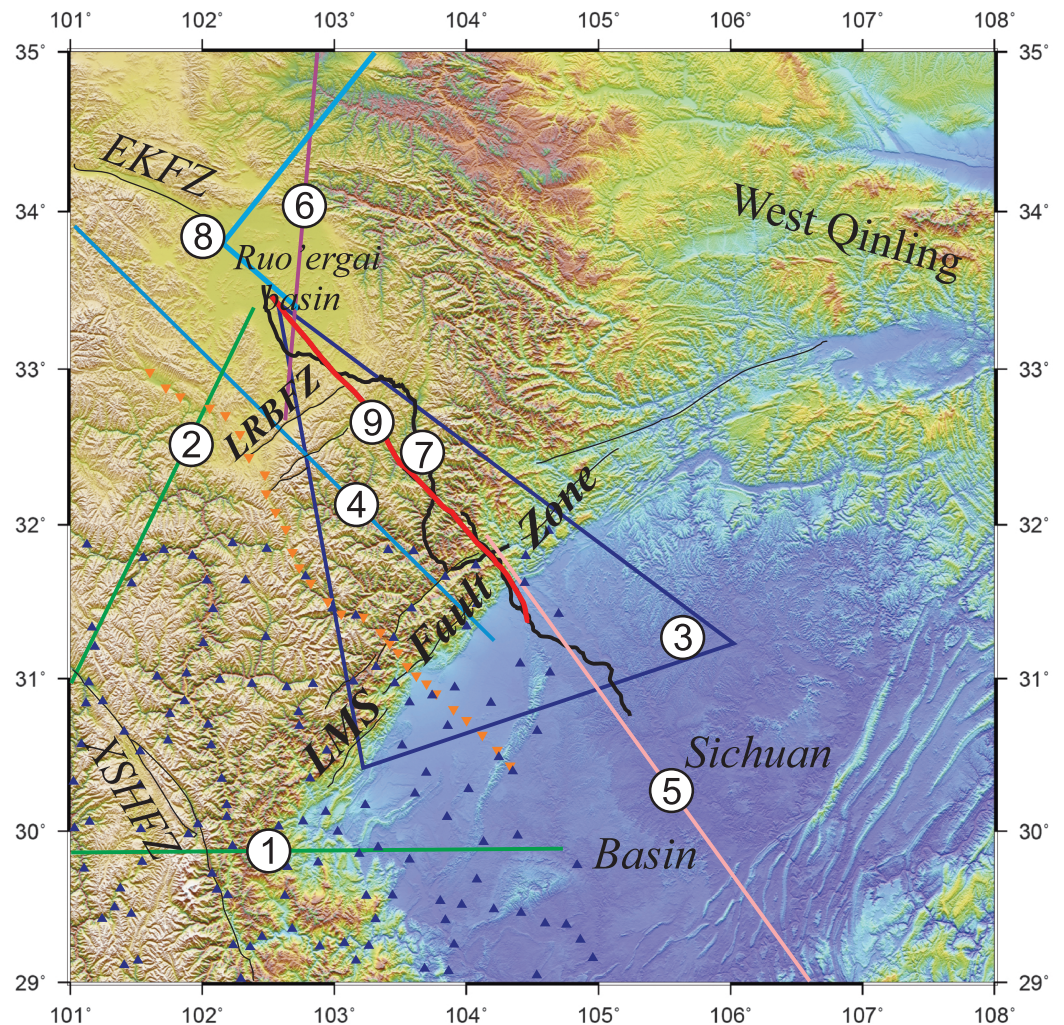


Figure 3. Locations of existing seismic experiments in the eastern Tibetan Plateau: (1) Batang-Zizhong profile, (2) Benzilan-Tangke profile, (3) Longmen Shan triangle, (4) GGT Altai-Taiwan profile (Altyntagh-Longmen Shan), (5) GGT Altai-Taiwan profile (Heishui-Shaoyang), (6) Ma'erkang-Gulang profile, (7) SinoProbe-02 seismic refraction profile, (8) Ruo'ergai deep seismic reflection profile, and (9) SinoProbe-02 deep seismic reflection profile. The orange inverted triangles represent the passive seismic array of Zhang *et al.* [2010]; the blue triangles represent the passive seismic array of Liu *et al.* [2008].

Although recognition of the Yangtze crystalline basement beneath easternmost Tibet has provided significant constraints on understanding the tectonic features of the Longriba fault zone, precisely how far the Yangtze block extends westward remains ambiguous, and whether the western margin of the Yangtze block coincides with the Longriba fault zone has not been fully discussed.

3. Delineation of the Longriba Fault Zone

3.1. Structural Distribution of the Longriba Fault Zone at the Surface

The Longriba fault zone is an active feature [Shen *et al.*, 2005; Xu *et al.*, 2008; Ren *et al.*, 2013a, 2013b], but the mechanism for its initiation is not fully understood. In addition, the extent of this fault zone to the southwest still remains ambiguous due to the extreme topography, and differing interpretations of its extent have been proposed [Xu *et al.*, 2008; Ren *et al.*, 2013a, 2013b]. Thus, our understanding of the tectonic significance of the Longriba fault zone, as well as the kinematic response of eastern Tibet to the ongoing India-Eurasia collision, is limited.

In this study, we employed PALSAR (Phased Array type L-band Synthetic Aperture Radar) images provided by the ALOS (Advanced Land Observing Satellite) from the Japan Aerospace Exploration Agency to delineate the

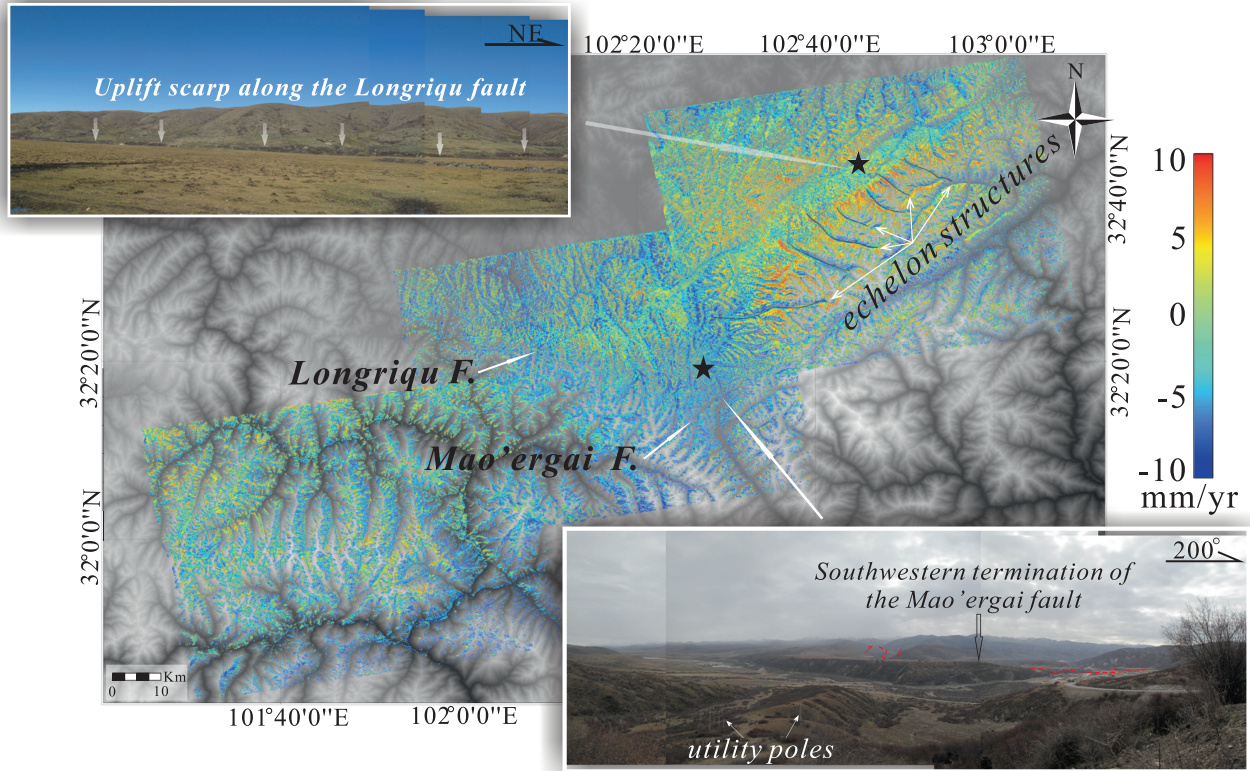


Figure 4. Map of mean LOS velocities (in mm/yr) along the Longriba fault zone and adjacent areas between January 2007 and February 2010 derived from ALOS PALSAR data. The field images on the top left and bottom right corner capture the scarp of the Longriqu fault (white arrows) and the southwestern termination of the Mao'ergai fault zone (red dashed lines), respectively. The stars indicate the points where the pictures were taken. Please refer to Figure 1 for the geographic location.

general linear patterns of geologic structures and to investigate the surface structures and extent of the dextral transpressive Longriba fault zone (Figure 4). In our study area, we were able to obtain 12 L-band (23.6 cm) ALOS acquisitions over the period of 2007–2011 that were available along ascending paths that cover most of the Longriba fault zone and the areas to the southwest. HH (horizontal-horizontal) polarization mode data were chosen for the synthetic aperture radar (SAR) data for better performance [e.g., Cloude and Papathanassiou, 1998]. All SAR interferograms are processed using GAMMA software [Werner et al., 2000]. Additionally, in order to correct the phase due to topography, the 90 m Shuttle Radar Topography Mission digital elevation model is used. Using our ALOS-PALSAR data set, conventional interferometric synthetic aperture radar (InSAR) analysis is able to generate differential interferograms covering 4 years with a high coherence not only in the Longriba fault zone but also the areas to the southwest. The quality of these interferograms makes precise mapping of a clear phase discontinuity possible, and it is coincident with the previously mapped Longriba fault zone.

The mean line-of-sight (LOS) velocity pattern was employed to investigate the rate of surface displacement in association with the eastward extrusion of the Tibetan Plateau and, correspondingly, to delineate the spatial response along the Longriba fault zone (Figure 4). Please refer to Tables 2 and 3 for detailed information on the parameters about the PALSAR data.

Two areas of ground displacement can be distinguished in the mean LOS velocity map: the northeastern area around the Longriba fault zone and the area to the southwest (Figure 4). Surface displacement in association with the Longriqu fault and the Mao'ergai fault is clearly visible in the study area (Figure 4). Differential movement rates are evident on both sides of the Longriqu fault (Figure 4). The positive LOS values located on the northwestern, hanging wall of the Longriqu fault and the mostly negative LOS values located on the southeastern, the footwall, are compatible with thrusting at a rate of ~6–8 mm/yr in the period of 2007–2011 (Figure 4). Field images capture the fault scarp in association with thrusting along the Longriqu

Table 2. PALSAR Data Parameters

| Acquisition Mode | Processing Level | Acquisition Time | | | Polarization | Incidence Angle (deg) | Antenna Size (m) |
|------------------|------------------|------------------|------------|------------|--------------|-----------------------|--|
| | | Track 1 | Track 2 | Track 3 | | | |
| FBS ^a | 1.1 | 20,070,207 | 20,070,121 | 20,070,219 | HH | 38.7158 | Azimuth: 4.684257 Elevation: 3.152046 |
| | | 20,080,210 | 20,080,124 | 20,080,222 | | | |
| | | 20,100,215 | 02,100,129 | 20,100,112 | | | |
| | | 20,110,103 | 201,102,01 | 20,110,115 | | | |

^aFine beam single polarization.

fault zone (inset in Figure 4 (top left)). To the east, no obvious LOS velocity changes were observed across the Mao’ergai fault. Previous studies have established structural features of the Mao’ergai fault and that dextral strike-slip shearing is present [Xu *et al.*, 2008; Ren *et al.*, 2013a]. Although there is no obvious evidence shown in the mean LOS velocity map, the NW striking en echelon structures situated between the Longriqu and Mao’ergai faults (Figure 4) can be viewed as an accommodation of the dextral strike-slip shearing along the Mao’ergai fault.

The small NE-SW gradients of LOS mean velocity along the southwestern tips of the Longriqu and Mao’ergai faults (short white arrows in Figure 4) appear to define the southwestern termination of the Longriba fault zone. Farther southwest, the mean LOS velocity map indicates that no obvious localized surface displacement is present (Figure 4).

Overall, our interpretation and analysis of the mean LOS velocity image suggests that the extent of the Longriba fault zone terminates before reaching the Xianshuihe fault zone. Our analysis strongly indicates that the Longriba fault zone is the key structure responsible for the observed sharp gradient in GPS velocities. In addition, these scenarios are consistent with the surface expression at its southwestern end of the Longriba fault zone being perpendicular to the Triassic anticlines, cutting through their eastern portion discontinuously (Figure 1). Field images taken in the southwestern tip of the Mao’ergai fault provide additional supports that the Mao’ergai fault is truncated against the Triassic anticlines at its southwest end (inset in Figure 4 (bottom right)). Farther southwest, the Triassic anticlines are continuous and subperpendicular to the Longmen Shan fault zone [Wang *et al.*, 2001; Wang and Meng, 2009], indicating the termination of the Longriba fault zone (Figure 1).

3.2. Constitution of the Longriba Fault Zone at Depth

The southeastern segment of the NW-SE trending Ruo’ergai seismic reflection line (~65 km) overlaps with the northwestern portion of the SinoProbe-02 Longmen Shan line (~310 km). Therefore, for the purpose of this study, we included the published results of the NW-SE trending seismic line from Wang *et al.* [2011] (section I in Figure 5) and Guo *et al.* [2013] (section II in Figure 5) together to document the structural variations across the Longriba fault zone (Figures 3 and 5) and the nature of the Longriba fault zone at depth. First of all, the topography on opposite sides of the Longriba fault zone is different, having low relief in the Ruo’ergai basin and very high relief to the southeast (Figure 5). Additionally, complex intracrustal reflectors extend to the Moho beneath the Ruo’ergai basin (section I in Figure 5). These intracrustal reflectors are strong and similar in nature so that the bottom of the sedimentary cover cannot be clearly delineated (section I in Figure 5). However, to the southeast of the Longriba fault zone, the crustal reflectivity is totally different (section II in Figure 5). Two discrete boundaries that are the top of the

Table 3. Main Parameters Used in InSAR Processing

| Track 1 | | | Track 2 | | | Track 3 | | |
|-----------------------|--------------------|------------|-----------------------|--------------------|------------|-----------------------|--------------------|------------|
| Acquisition Time | Time Interval/Year | Baseline/m | Acquisition Time | Time interval/Year | Baseline/m | Acquisition Time | Time Interval/Year | Baseline/m |
| 20,070,207–20,080,210 | 1 | 1972.2 | 20,070,121–20,080,124 | 1 | 3114.6 | 20,070,219–20,080,222 | 1 | 1478.3 |
| 20,080,210–20,100,215 | 2 | 861.9 | 20,080,124–20,100,129 | 2 | –682.5 | 20,080,222–20100112 | 2 | –1459.8 |
| 20,100,215–20,110,103 | 1 | 1203.4 | 20,100,129–20,110,201 | 1 | 1615.9 | 20,100,112–20,110,115 | 1 | 1910.9 |

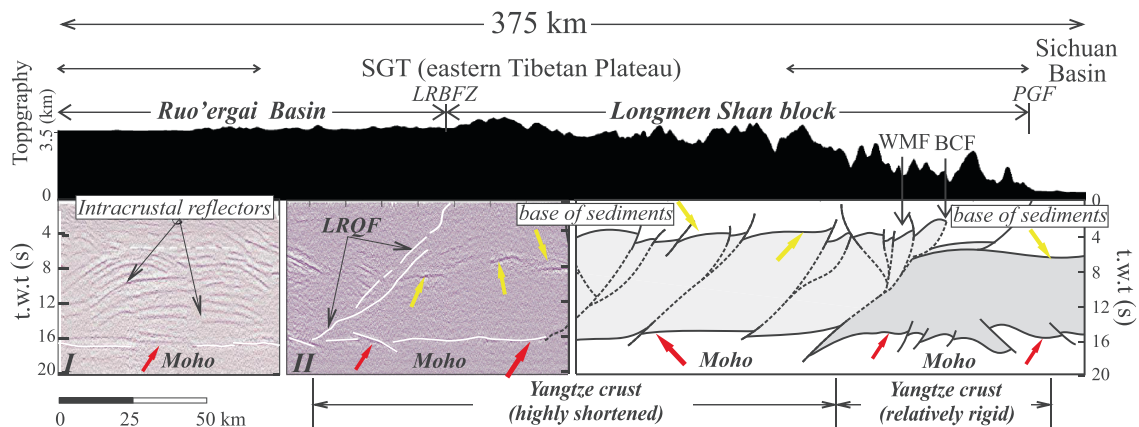


Figure 5. Available seismic reflection images [Wang et al., 2011; Guo et al., 2014] on both sides of the Longriba fault zone and interpreted results regarding the crustal structure beneath easternmost Tibet: SGT = Songpan-Ganzi terrane, LRBFZ = LRQF = Longriqua fault Longriba fault zone, PGF = Pengguan fault, WMF = Wenchuan-Maowen fault, and BCF = Beichuan fault.

basement and the crust-mantle boundary (Moho) can be identified (section II in Figure 5) [Guo et al., 2013, 2014]. In addition, the intracrustal reflectivity is not as well developed as that beneath the Ruo'ergai basin.

Guo et al. [2013, 2014] infer the existence of the Yangtze crystalline crust beneath easternmost Tibet (Figure 5). The crust has been highly shortened beneath the easternmost Tibetan Plateau but displays relatively similar properties to the Sichuan basin (Figure 5). Shortening of the Yangtze crystalline crust and its overlying sediments resulted in a higher topographic relief than that of the area west of the Longriba fault zone where the Yangtze crystalline crust is absent. In addition, viewing the seismic results in a regional perspective along with the gravity and magnetic anomalies, Guo et al. [2014] concluded that the western margin of the Yangtze lithospheric block extends beyond the LMS block in the northeast and merges gradually with the LMS block to the southwest. As discussed below, this irregular western margin of the Yangtze block beneath easternmost Tibet provides significant constraints on interpretations of the tectonic nature of the Longriba fault zone.

Regarding the onset of this fault zone, although there is no precise dating data to constrain the initiation of the Longriba fault zone, the youngest depositing time of the terrace that was offset by the Mao'ergai fault is dated to be 75 ka by optically stimulated luminescence method [Xu et al., 2008], indicating that the Longriba fault zone is a newly generated fault zone that probably initiated in the late Quaternary.

4. Discussion and Interpretation

In this study, together with the new documentation that the Longriba fault zone does not appear to reach the Xianshuihe fault zone that is well to the southwest, integrated geological and geochemical studies indicated an irregular western margin of the Yangtze block, which is consistent with previous studies by Guo et al. [2014]. Thus, reviewing these results regarding the preexisting structure of the lithosphere that was acquired from tectonic inheritance of the Songpan-Ganzi terrane and adjacent areas, we constructed a 3-D block diagram to elucidate the crustal structure beneath easternmost Tibet (Figure 6a). This 3-D image illustrates that the western margin of the Yangtze crystalline basement (Yangtze block, YB) extends to the northwest beyond the Longmen Shan (LMS) fault zone to the Longriba fault zone. The regional crustal thickness is about 50–55 km. To the southwest, however, the western margin of the YB gradually merges with the LMS fault zone (Figures 6a and 6b), and the crustal thickness has reached 55–60 km in this area. This variation from northeast to southwest indicates that the collision in the south between the Songpan-Ganzi terrane and the Sichuan basin (western YB) is absorbed by crustal thickening due to weaker structural integrity than that of the area to the northeast where the Yangtze block is present. In addition, this interpretation also explains why the Yangtze-type Sinian and Paleozoic strata are exposed only in the northern portion of the Songpan-Ganzi terrane (Figure 1).

The trend of the fold axes of the Triassic flysch sediments (Figures 1 and 6b), as well as the eastward escape of the Tibetan Plateau as detected by GPS data [Shen et al., 2005], would have been significantly affected by the

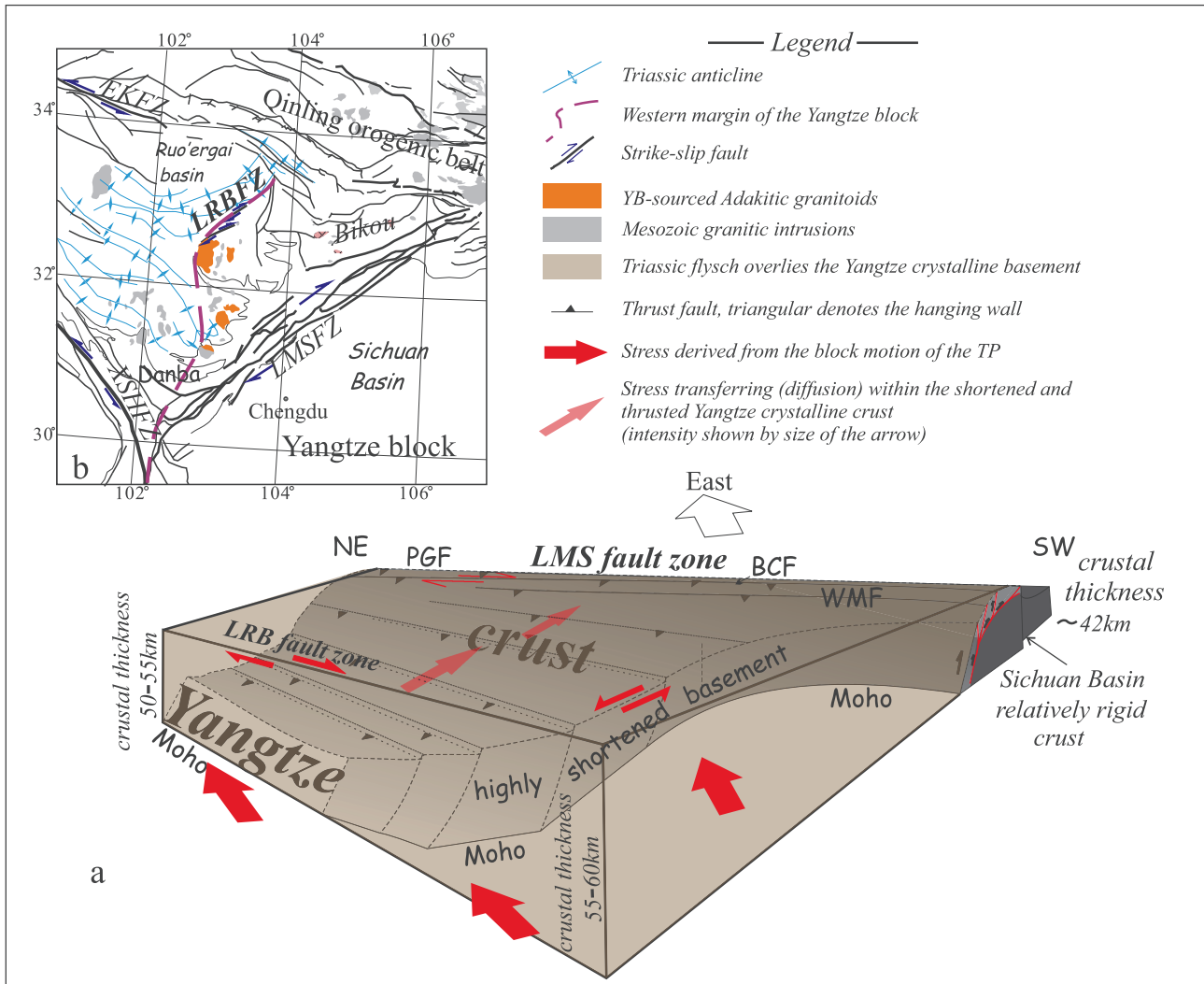


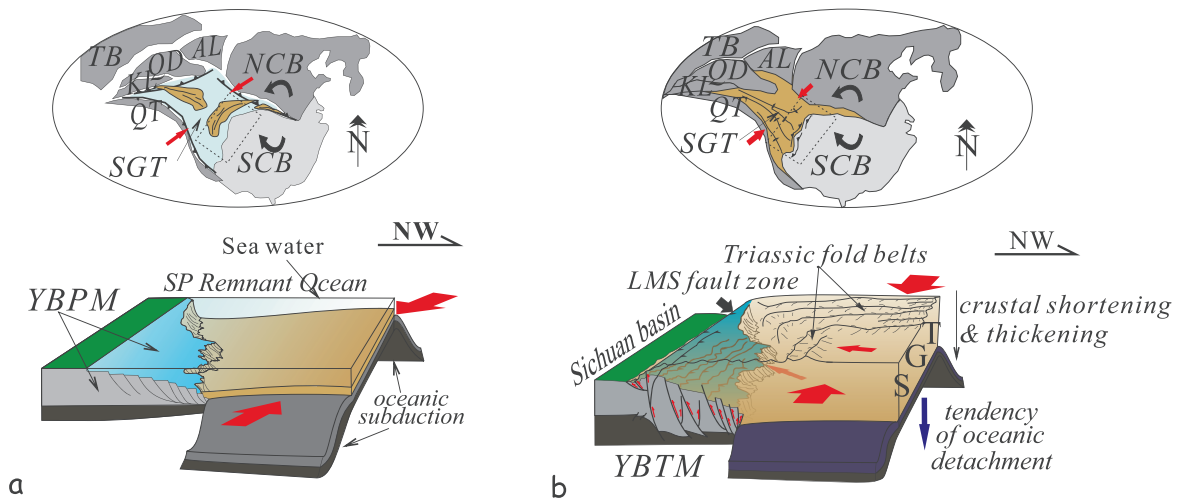
Figure 6. (a) Simplified lateral heterogeneity of the western margin of the Yangtze crystalline basement beneath the easternmost Tibetan Plateau (as shown in the shaded area), looking east. (b) Spatial distribution of the western margin of the YB in a map view: LMS = Longmen Shan, LRB = Longriba fault, PGF = Pengguan fault, BCF = Beichuan fault, and WMF = Wenchuan-Maowen fault.

existing crystalline continental basement beneath eastern Tibet. The highly shortened Yangtze crystalline basement beneath the eastern edge of Tibet is mostly attributed to the intense southeastward directed thrusting during the Triassic. The Cenozoic eastward block extrusion of the eastern Tibetan Plateau would have probably reactivated the previously shortened western Yangtze crust and generated uplift of the eastern edge of Tibet.

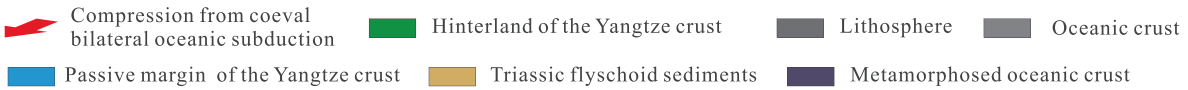
Based on the geologic and geophysical constraints from the eastern Tibetan plateau, we propose that the Longriba fault in the northeastern Songpan-Ganzi terrane marks the westernmost edge of the Yangtze block. We further propose a general evolutionary model with respect to the tectonic interactions between the eastern Songpan-Ganzi terrane and western YB for the interval from the Mesozoic to Quaternary (Figure 7). During the onset of the Indosinian orogeny, coeval bilateral subduction along the north and southwest margins of the Songpan-Ganzi paleo-oceanic basin, as well as progressive deposition of the Triassic flyschoid sedimentary rocks, led to closure of the Songpan-Ganzi Remnant Ocean and growth of the Songpan accretionary prism (Figure 7a). Subsequently, crustal shortening and thickening occurred. As a result, thrusting took place toward the southeast, i.e., toward the passive margin of the YB (Figure 7b). The Indosinian deformation events generated fold belts of the Triassic strata and sinistral transpressive movement along LMS fault zone. The passive margin of the western YB was also reactivated and highly

Indosinian orogeny (Early Triassic)

Indosinian orogeny (Mid Triassic)

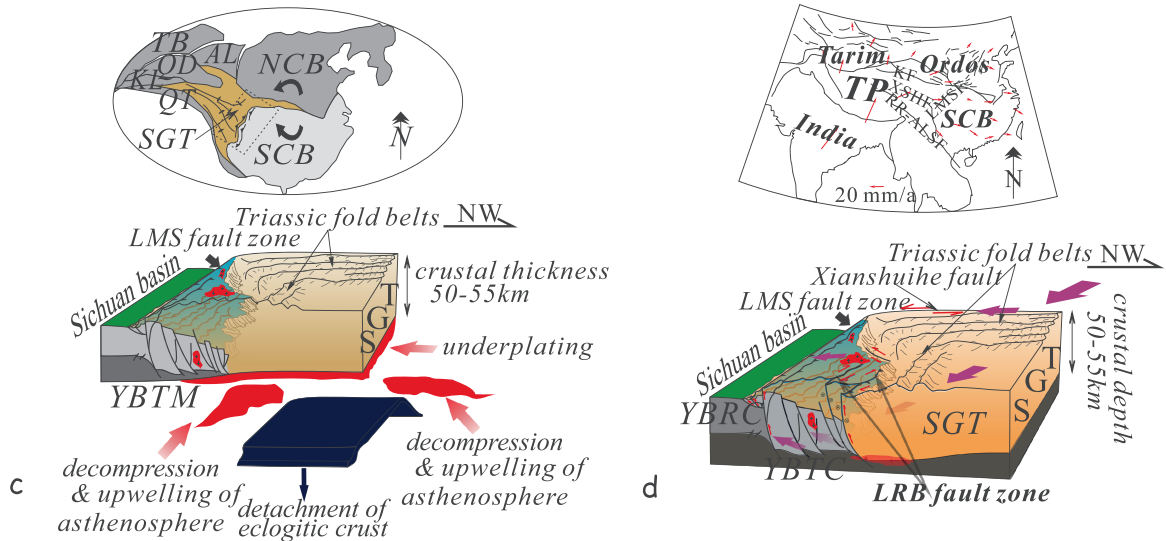


Legend



Indosinian orogeny (Late Triassic-Early Jurassic)

Neotectonics (since ~55Ma)



Legend

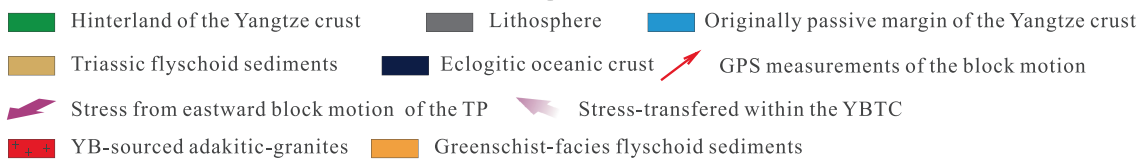


Figure 7. Sketch of the tectonic interactions between the Songpan-Ganzi terrane and adjacent areas during the (a) Early Triassic to (b) Middle Triassic and the time period during the (c) Late Triassic to (d) Quaternary: NCB = north China block, SCB = south China block, TB = Tarim basin, QB = Qaidam basin, AL = Alxa League, QT = Qiangtang terrain, YBPM = passive margin of Yangtze block, YBTM = thrust margin of the Yangtze block, SGT = Songpan-Ganzi terrane, TP = Tibetan Plateau, LMS = Longmen Shan, and LRB = Longriba fault.

shortened (Figure 7b). However, due to the irregular western margin of the Yangtze crust, fold axes of the Triassic series strike NW-SE in the southern Songpan-Ganzi terrane, which are nearly perpendicular to the LMS fault zone. These fold axes change to strike NE-SW, which is parallel to the Longriba and LMS fault zones in the northern Songpan-Ganzi terrane (Figures 6b and 7b). At this point, the contemporaneous sinistral East Kunlun strike-slip fault [Li, 1996; Weislogel, 2008] might have provided the stress for the formation of NE-SW striking fold belts (Figure 6b). Triassic fold belts with vertical axial planes can be continuously mapped for several tens of kilometers (Figure 6b).

Later during the Indosinian orogeny, the deep sediment-filled Songpan-Ganzi Remnant Ocean prevented a complete continent-continent collision during divergent double subduction [Soesoo *et al.*, 1997], but the crust thickened due to deformation. As a result, detachment of the oceanic plate from the overlying accretionary prism occurred as a result of metamorphism of basaltic crust to eclogitic crust after the overlying crust thickened to more than 50 km [Hacker, 1996] (Figure 7c). This hypothesis is consistent with previous studies that indicate that the crustal thickness of the NE Tibetan Plateau reached ~50 km prior to ~55 Ma [Zhang *et al.*, 2006; Lease *et al.*, 2012]. Consequently, downward movement of the oceanic slab resulted in upwelling of the asthenosphere, which then mixed with mantle wedges (Figure 7c). Underplating beneath both the lower crust of the Yangtze western margin and Songpan accretionary prism caused partial melting, which generated Yangtze block-sourced adakitic-type granitoids in the easternmost Songpan-Ganzi terrane between the Longriba and the LMS fault zones (Figures 6b and 7c).

Today, the Tibetan Plateau is undergoing eastward block motion as a response to the ongoing Himalayan orogeny. In the Songpan-Ganzi terrane, some of the stresses have been absorbed by highly shortened Yangtze crust beneath the easternmost Songpan-Ganzi terrane, and the block motion rate drops dramatically as a consequence (Figure 7d). The dextral transpressive Longriba fault zone was therefore generated along this tectonic system as an accommodation of the differential kinematic movements (Figure 7d). In addition, owing to absorbance and resistance of the western margin of the Sichuan basin, less stress reaches the LMS fault zone, which accounts for the <3 mm/yr slip rate and a lack of historically recorded major earthquakes ($M_s > 7$) before 2008 along it. Thus, recognition of the western margin of the YB, as well as the tectonic significance of the Longriba fault zone, is a key to addressing several fundamental questions about the eastern Tibet region.

5. Conclusions

In this paper, together with review and summary of available geological and geophysical constraints regarding the tectonic interactions of the Songpan-Ganzi terrane with the Yangtze block since the Early Mesozoic, we employed ALOS-PALSAR data to delineate the spatial extent of the Longriba fault zone at the surface. The following lines of evidence lead us to conclude that the Longriba fault zone, instead of the Longmen Shan fault zone, marks the westernmost edge of the Yangtze crustal block: (a) a sharp GPS velocity gradient along the Longriba fault zone, (b) localized distribution of the YB-sourced adakitic granitoids, (c) direct evidence from the seismic reflection image and other geophysical data, (d) the spatial extent of the Longriba fault zone at the surface, and (e) the continuous distribution of the Triassic flysch anticlines around the western margin of the Yangtze crystalline basement. The newly identified western edge of the Yangtze block implies a paleocontinent-ocean boundary at depth. This boundary is a potential weak zone. Ongoing eastward extrusion of the eastern Tibetan Plateau has worked on this preexisting structure of the lithosphere that was acquired from the regional tectonic inheritance and finally recorded the traces of the western edge of the YB at the surface. The results of this paper should advance our understanding of the tectonic relationship between the Songpan-Ganzi terrane and Yangtze block and further provide extra constraints for the geodynamic response of eastern Tibet to the ongoing India-Eurasia collision.

References

- Arne, D., B. Worley, C. Wilson, S.F. Chen, D. Foster, Z. L. Luo, S. G. Liu, and P. Dirks (1997), Differential exhumation in response to episodic thrusting along the eastern margin of the Tibetan Plateau, *Tectonophysics*, 280, 239–256.
- Avigad, D. (1995), Exhumation of the Dabie Shan ultra-high-pressure rocks and accumulation of the Songpan-Ganzi flysch sequence, central China: Comment and reply, *Geology*, 23, 764–765.
- Burchfiel, B. C., and Z. L. Chen (2012), Tectonics of the southeastern Tibetan Plateau and its adjacent foreland, *Geol. Soc. Am. Mem.*, 210, 1–164.
- Burchfiel, B. C., Z. L. Chen, Y. P. Liu, and L. H. Royden (1995), Tectonics of the Longmen Shan and adjacent regions, central China, *Int. Geol. Rev.*, 37, 661–735.

Acknowledgments

We would like to acknowledge Lindsay Schoenbohm and the anonymous reviewers for their valuable comments on earlier versions of this manuscript. ALOS-PALSAR data were obtained from the Japan Aerospace Exploration Agency (<http://global.jaxa.jp/>) through a National Natural Science Foundation of China grant (41304064). This work was supported by the SinoProbe-02 Project, National Natural Science Foundation of China grants (41430213, 41304064, 41174081, 41190072, and 41325009) and a U.S. National Science Foundation, Partnerships for International Research and Education grant (0730154). We would like to acknowledge J. Encarnación at Saint Louis University for his valuable comments on earlier version of this manuscript.

- Chang, E. Z. (2000), Geology and tectonics of the Songpan-Ganzi fold belt, southwestern China, *Int. Geol. Rev.*, *42*, 813–831.
- Chen, S. F., C. J. L. Wilson, Q. D. Deng, X. L. Zhao, and Z. L. Luo (1994), Active faulting and block movement associated with large earthquakes in the Min Shan and Longmen Mountains, northeastern Tibetan Plateau, *J. Geophys. Res.*, *99*(B12), 24,025–24,038, doi:10.1029/94JB02132.
- Chen, X. B., Y. Q. Wu, and P. S. Du (1988), The characteristics of velocity structure on the two sides of Longmen Shan fault zone, in *Development on the Research of Deep Structures of China's Continent* [in Chinese], edited by Department of Scientific Monitoring, China Seismological Bureau, pp. 97–113, Geol. Press, Beijing.
- Chen, Z., B. C. Burchfiel, Y. Liu, R. W. King, L. H. Royden, W. Tang, E. Wang, J. Zhao, and X. Zhang (2000), Global Positioning System measurements from eastern Tibet and their implications for India/Eurasia intercontinental deformation, *J. Geophys. Res.*, *105*, 16,215–16,227, doi:10.1029/2000JB900092.
- Clark, M. K., M. A. House, L. H. Royden, K. X. Whipple, B. C. Burchfiel, X. Zhang, and W. Tang (2005), Late Cenozoic uplift of southeastern Tibet, *Geology*, *33*, 525–528.
- Cloude, S. R., and K. P. Papathanassiou (1998), Polarimetric SAR interferometry, *IEEE Trans. Geosci. Rem. Sens.*, *36*, 1551–1565.
- Cui, Z. Z., J. P., Chen, and L. Wu (1996), *Synthetic Study on Lithospheric Geoscience Section From Altai to Taiwan: Deep Structure and Tectonics Along Huashixia-Shaoyang Profile* [in Chinese], pp. 49–168, Geol. Press, Beijing.
- Dewey, J. F., R. M. Shackleton, C. F. Chang, and Y. Y. Sun (1988), The tectonic evolution of the Tibetan Plateau, *Phil. Trans. R. Soc. Lond. A*, *327*, 379–413.
- Enkelmann, E., L. Ratschbacher, R. Jonckheere, R. Nestler, M. Fleischer, R. Gloaguen, B. R. Hacker, Y. Q. Zhang, and Y. S. Ma (2006), Cenozoic exhumation and deformation of northeastern Tibet and the Qinling: Is Tibetan lower crustal flow diverging around the Sichuan Basin?, *Geol. Soc. Am. Bull.*, *118*, 651–671, doi:10.1130/B25805.1.
- Enkelmann, E., A. Weislogel, L. Ratschbacher, E. Eide, A. Renno, and J. Wodden (2007), How was the Triassic Songpan-Ganzi basin filled? A provenance study, *Tectonics*, *26*, TC4007, doi:10.1029/2006TC002078.
- Gan, W. J., P. Z. Zhang, Z. K. Shen, Z. J. Niu, M. Wang, Y. G. Wan, D. M. Zhou, and J. Cheng (2007), Present-day crustal motion within the Tibetan Plateau inferred from GPS measurements, *J. Geophys. Res.*, *112*, B08416, doi:10.1029/2005JB004120.
- Gao, R., Z. W. Lu, Q. S. Li, Y. Guan, J. S. Zhang, R. Z. He, and L. Y. Huang (2005), Geophysical survey and geodynamic study of the crust and upper mantle in the Qinghai-Tibet Plateau, China, *Episodes*, *28*, 263–273.
- Guo, X. Y., J. Encarnacion, X. Xu, A. Deino, Z. W. Li, and X. B. Tian (2012), Collision and rotation of the south China block and their role in the formation and exhumation of ultrahigh pressure rocks in the Dabie Shan orogen, *Terra Nova*, *24*, 339–350.
- Guo, X. Y., R. Gao, G. R. Keller, X. Xu, H. Y. Wang, and W. H. Li (2013), Imaging the crustal structure beneath eastern Tibet and implications for the uplift of Longmen Shan range, *Earth Planet. Sci. Lett.*, *379*, 72–80.
- Guo, X. Y., G. R. Keller, R. Gao, X. Xu, H. Y. Wang, and W. H. Li (2014), Irregular western margin of the Yangtze block as a cause of variation in tectonic activity along the Longmen Shan fault zone, eastern Tibet, *Int. Geol. Rev.*, *56*, 473–480.
- Hacker, B. R. (1996), Eclogite formation and the rheology, buoyancy, seismicity, and H₂O content of oceanic crust, *AGU Monogr.*, *337*–346.
- Harrowfield, M. J., and C. J. L. Wilson (2005), Indosinian deformation of the Songpan Garzê Fold Belt, northeast Tibetan Plateau, *J. Struct. Geol.*, *27*, 101–117.
- Huang, J., and B. Chen (1987), *The Evolution of the Tethys in China and Adjacent Regions*, Geological House, Beijing.
- Jolivet, M., M. Brunel, D. Seward, Z. Xu, J. Yang, J. Malavieille, F. Roger, A. Leyreloup, N. Arnaud, and C. Wu (2003), Neogene extension and volcanism in the Kunlun fault zone, northern Tibet: New constraints on the age of the Kunlun fault, *Tectonics*, *22*(10), 1052, doi:10.1029/2002TC001428.
- King, R. W., F. Shen, B. C. Burchfiel, L. H. Royden, E. Wang, Z. Chen, Y. Liu, X. Zhang, J. Zhao, and Y. Li (1997), Geodetic measurements of crustal motion in southwest China, *Geology*, *25*, 179–182.
- Kirby, E. (2008), Geomorphic insights into the growth of eastern Tibet and implications for the recurrence of great earthquakes, *AGU*, *89*, Fall Meet. Suppl., Abstract T24B-03.
- Kirby, E., P. W. Reiners, M. A. Krol, K. X. Whipple, K. V. Hodges, K. A. Farley, W. Q. Tang, and Z. L. Chen (2002), Late Cenozoic evolution of the eastern margin of the Tibetan Plateau: Inferences from Ar/Ar and (U-Th)/He thermochronology, *Tectonics*, *21*(1), 1001, doi:10.1029/2000TC001246.
- Kirby, E., N. Harkins, E. Wang, X. H. Shi, C. Fan, and D. Burbank (2007), Slip rate gradients along the eastern Kunlun fault, *Tectonics*, *26*, TC2010, doi:10.1029/2006TC002033.
- Lease, R. O., D. W. Burbank, H. P. Zhang, J. H. Liu, and D. Y. Yuan (2012), Cenozoic shortening budget for the northeastern edge of the Tibetan Plateau: Is lower crustal flow necessary?, *Tectonics*, *31*, TC3011, doi:10.1029/2011TC003066.
- Li, S., W. D. Mooney, and J. Fan (2006), Crustal structure of mainland China from deep seismic sounding data, *Tectonophysics*, *420*, 239–252.
- Li, T. D. (Ed.) (1996), *Geologic Map of the Qinling-Daba Mountains and Adjacent Regions of the People's Republic of China*, Chinese Academy of Geological Sciences, Geologic House, Scale 1: 1,000,000.
- Li, Z. C., X. Z. Pei, S. P. Ding, Z. Q. Liu, F. Wang, G. Y. Li, R. B. Li, and F. J. Li (2007), Zircon U-Pb dating of the Nanyili granodiorite in the Pingwu area, northwestern Sichuan, and its geological significance, *Geol. China*, *24*, 1003–1012.
- Liu, Q. Y., J. H. Chen, S. C. Li, Y. Li, B. Guo, J. Wang, and S. H. Qi (2008), The M_s 8.0 Wenchuan earthquake: Preliminary results from the western Sichuan mobile seismic array observations [in Chinese with English abstract], *Seismol. Geol.*, *30*, 584–596.
- Lu, S., D. P. Yan, Y. Wang, J. F. Gao, and L. Qi (2010), Geochemical and geochronological constraints on the Mashan and Mupi plutons in the south Qinling orogenic belt: Implications for tectonic nature of the Bikou terrane [in Chinese with English abstract], *Acta Petrol. Sin.*, *26*, 1889–1901.
- Lv, J. N., Z. K. Shen, and M. Wang (2003), Contemporary crustal deformation and active tectonic block model of the Sichuan-Yunnan region, China [in Chinese with English abstract], *Seismol. Geol.*, *25*, 543–554.
- Maniar, P. D., and P. M. Piccoli (1989), Tectonic discrimination of granitoids, *Geol. Soc. Am. Bull.*, *101*, 635–643.
- Meng, Q. R., E. Wang, and J. M. Hu (2005), Mesozoic sedimentary evolution of the northwest Sichuan basin: Implication for continued clockwise rotation of the south China block, *Geol. Soc. Am. Bull.*, *117*, 396–410.
- Molnar, P., and K. E. Dayem (2010), Major intracontinental strike-slip faults and contrasts in lithospheric strength, *Geosphere*, *6*, 444–467.
- Nalbant, S. S., and J. McCloskey (2011), Stress evolution before and after the 2008 Wenchuan, China earthquake, *Earth Planet. Sci. Lett.*, *307*, 222–232.
- Nie, S., A. Yin, D. B. Rowley, and Y. Jin (1994), Exhumation of the Dabie Shan ultra-high-pressure rocks and accumulation of the Songpan-Ganzi flysch sequence, central China, *Geology*, *22*, 999–1002.
- Ouimet, W., K. Whipple, L. Royden, P. Reiners, K. Hodges, and M. Pringle (2010), Regional incision of the eastern margin of the Tibetan Plateau, *Lithosphere*, *2*, 50–63.
- Pullen, A., P. Kapp, G. Gehrels, J. D. Vervoot, and L. Ding (2008), Triassic continental subduction in central Tibet and Mediterranean-style closure of the Paleo-Tethys Ocean, *Geology*, *36*, 351–354.

- Reid, A. J., C. J. L. Wilson, and S. Liu (2005), Structural evidence for the Permo-Triassic tectonic evolution of the Yidun arc, eastern Tibetan Plateau, *J. Struct. Geol.*, *27*, 119–137.
- Reid, A. J., C. J. L. Wilson, S. Liu, N. Pearson, and E. Belousova (2007), Mesozoic plutons of the Yidun arc, SW China: U/Pb geochronology and Hf isotopic signature, *Ore Geol. Rev.*, *31*, 88–106.
- Ren, J. J., X. W. Xu, R. S. Yeats, and S. M. Zhang (2013a), Latest Quaternary paleoseismology and slip rates of the Longriba fault zone, eastern Tibet: Implications for fault behavior and strain partitioning, *Tectonics*, *32*, 216–238, doi:10.1002/tect.20029.
- Ren, J. J., X. W. Xu, R. S. Yeats, S. M. Zhang, R. Ding, and Z. Gong (2013b), Holocene paleoearthquakes of the Maoergai fault, eastern Tibet, *Tectonophysics*, *590*, 121–135.
- Roger, F., J. Malavieille, P. H. Leloup, S. Calassou, and Z. Xu (2004), Timing of granite emplacement and cooling in the Songpan-Ganzi fold belt (eastern Tibetan Plateau) with tectonic implications, *J. Asian Earth Sci.*, *22*, 465–481.
- Roger, F., M. Jolivet, and J. Malavieille (2010), The tectonic evolution of the Songpan-Ganzé (north Tibet) and adjacent areas from Proterozoic to present: A synthesis, *J. Asian Earth Sci.*, *39*, 254–269.
- Roger, F., M. Jolivet, R. Cattin, and J. Malavieille (2011), Mesozoic-Cenozoic tectonothermal evolution of the eastern part of the Tibetan Plateau (Songpan-Ganze, Longmen Shan area): Insights from thermochronological data and simple thermal modeling, in *Growth and Collapse of the Tibetan Plateau*, edited by R. Gloaguen and L. Ratschbacher, *Geol. Soc. London Spec. Publ.*, *353*, 9–25.
- Shen, Z. K., J. N. Lü, M. Wang, and R. Bürgmann (2005), Contemporary crustal deformation around the southeast borderland of the Tibetan Plateau, *J. Geophys. Res.*, *110*, B11409, doi:10.1029/2004JB003421.
- Shen, Z. K., J. B. Sun, P. Z. Zhang, Y. G. Wan, M. Wang, R. Bürgmann, Y. H. Zeng, W. J. Gan, H. Liao, and Q. L. Wang (2009), Slip maxima at fault junctions and rupturing of barriers during the 2008 Wenchuan earthquake, *Nat. Geosci.*, *2*, 718–723, doi:10.1038/ngeo636.
- Soesoo, A., P. D. Bons, D. R. Gray, and D. A. Foster (1997), Divergent double subduction: Tectonic and petrologic consequences, *Geology*, *25*, 755–758.
- Sun, W. D., S. G. Li, Y. D. Chen, and Y. J. Li (2002), Timing of synorogenic granitoids in the south Qinling, central China: Constraints on the evolution of the Qinling-Dabie Shan orogenic belt, *J. Geol.*, *110*, 457–468.
- Tapponnier, P., Z. Q. Xu, F. Roger, B. Meyer, N. Arnaud, G. Wittlinger, and J. S. Yang (2001), Oblique stepwise rise and growth of the Tibetan Plateau, *Science*, *294*, 1671–1677.
- Taylor, M., and A. Yin (2009), Active structures of the Himalayan-Tibetan orogeny and their relationships to earthquake distribution, contemporary strain field, and Cenozoic volcanism, *Geosphere*, *5*, 199–214.
- Wang, C. S., R. Gao, A. Yin, H. Y. Wang, Y. X. Zhang, T. L. Guo, Q. S. Li, and Y. L. Li (2011), A midcrustal strain-transfer model for continental deformation: A new perspective from high-resolution deep seismic reflection profiling across NE Tibet, *Earth Planet. Sci. Lett.*, *306*, 279–288.
- Wang, C. Y., J. P. Wu, H. Lou, M. D. Zhou, and Z. M. Bai (2003a), *P* wave crustal velocity structure in western Sichuan and eastern Tibetan region, *Sci. China Earth Sci.*, *46*(Supp.), 254–265.
- Wang, C. Y., W. B. Han, J. P. Wu, H. Lou, and Z. M. Bai (2003b), Crustal structure beneath the Songpan-Ganze orogenic belt [in Chinese with English abstract], *Acta Seismol. Sin.*, *25*, 229–241.
- Wang, C. Y., L. P. Zhu, H. Lou, B. S. Huang, Z. X. Yao, and X. H. Luo (2010), Crustal thicknesses and Poisson's ratios in the eastern Tibetan Plateau and their tectonic implications, *J. Geophys. Res.*, *115*, B11301, doi:10.1029/2010JB007527.
- Wang, E. C., and Q. R. Meng (2009), Mesozoic and Cenozoic tectonic evolution of the Longmen Shan fault belt, *Sci. China*, *52*, 579–592.
- Wang, E. Q., Q. R. Meng, Z. L. Chen, and L. Z. Chen (2001), Early Mesozoic left-lateral movement along the Longmen Shan fault belt and its tectonic implications [in Chinese with English abstract], *Earth Sci. Front.*, *8*, 375–384.
- Wang, E., E. Kirby, K. P. Furlong, M. van Soest, G. Xu, X. Shi, P. J. J. Kamp, and K. V. Hodges (2012), Two-phase growth of high topography in eastern Tibet during the Cenozoic, *Nat. Geosci.*, doi:10.1038/NNGEO1538.
- Wang, H. Y., R. Gao, Y. S. Ma, X. Zhu, Q. S. Li, Z. Y. Kuang, P. W. Li, and Z. W. Lu (2007), Basin-range coupling and lithosphere structure between the Zoige and the west Qinling [in Chinese with English abstract], *Chin. J. Geophys.*, *50*, 472–481.
- Wang, Y. X., G. H. Han, M. Jiang, and X. C. Yuan (2004), Crustal structure along the geosciences transect from Altay to Altun Tagh [in Chinese with English abstract], *Chin. J. Geophys.*, *47*, 240–249.
- Wang, Y. X., W. D. Mooney, G. H. Han, X. C. Yuan, and M. Jiang (2005), Crustal *P* wave velocity structure from Altyn Tagh to Longmen mountains along the Taiwan-Altay geoscience transect [in Chinese with English abstract], *Chin. J. Geophys.*, *48*, 98–106.
- Weislogel, A. L. (2008), Tectonostratigraphic and geochronologic constraints on evolution of the northeast Paleotethys from the Songpan-Ganzi complex, central China, *Tectonophysics*, *451*, 331–345.
- Weislogel, A. L., S. A. Graham, E. Z. Chang, J. L. Wooden, G. E. Gehrels, and H. S. Yang (2006), Detrital zircon provenance of the Late Triassic Songpan-Ganzi complex: Sedimentary record of collision of the north and south China blocks, *Geology*, *34*, 97–100.
- Werner, C., U. Wegmüller, T. Strozzi, and A. Wiesmann (2000), GAMMA SAR and interferometric processing software, ERS-ENVISAT symposium, Gothenburg, Sweden, 16–20 Oct.
- Wilson, C. J. L., and A. P. Fowler (2011), Denudational response to surface uplift in east Tibet: Evidence from apatite fission-track thermochronology, *Geol. Soc. Am. Bull.*, *123*, 1966–1987.
- Xu, X. W., X. Z. Wen, G. H. Chen, and G. H. Yu (2008), Discovery of the Longriba fault zone in eastern Bayan Har Block, China and its tectonic implication, *Sci. China Earth Sci.*, *51*, 1209–1223.
- Yin, A. (2010a), Cenozoic tectonic evolution of Asia: A preliminary synthesis, *Tectonophysics*, *488*, 293–325.
- Yin, A. (2010b), A special issue on the great 12 May 2008 Wenchuan earthquake (M_w 7.9): Observations and unanswered questions, *Tectonophysics*, *491*, 1–9.
- Yin, A., and T. M. Harrison (2000), Geologic evolution of the Himalayan-Tibetan orogen, *Annu. Rev. Earth Planet. Sci.*, *28*, 211–280.
- Yin, A., and S. Nie (1993), An indentation model for north and south China collision and the development of the Tanlu and Honam fault systems, eastern Asia, *Tectonics*, *12*, 801–813, doi:10.1029/93TC00313.
- Yuan, C., M. F. Zhou, M. Sun, Y. J. Zhao, S. Wilde, X. P. Long, and D. P. Yan (2010), Triassic granitoids in the eastern Songpan Ganzi Fold Belt, SW China: Magmatic response to geodynamics of the deep lithosphere, *Earth Planet. Sci. Lett.*, *290*, 481–492.
- Yuan, H. H., and Z. L. Zhang (1994), A study of the chronology of granitoid rocks in Indosinian-Yanshan period at the west Longmen Mountains, in *Uplifting of Longmen Mountains and Formation and Evolution of Sichuan Basin*, edited by Z. Luo, pp. 330–337.
- Yuan, H. H., Z. L. Zhang, and P. Zhang (1991), The uplifting and cooling histories of the Laojungou granite in the western margin of the central section of the Longmen Mountains [in Chinese with English abstract], *J. Chengdu College Geol.*, *18*, 17–22.
- Zhang, H. F., L. Zhang, N. Harris, L. L. Jin, and H. L. Yuan (2006), U-Pb zircon ages, geochemical and isotopic compositions of granitoids in Songpan-Ganze fold belt, eastern Tibetan Plateau: Constraints on petrogenesis and tectonic evolution of the basement, *Contrib. Mineral. Petrol.*, *152*, 75–88.

- Zhang, H. F., L. Xiao, L. Zhang, H. L. Yuan, and L. L. Jin (2007a), Geochemical and Pb-Sr-Nd isotopic compositions of Indosinian granitoids from the Bikou block, northwest of the Yangtze plate: Constraints on petrogenesis, nature of deep crust and geodynamics, *Sci. China Earth Sci.*, *50*, 972–983.
- Zhang, H. F., R. Parrish, L. Zhang, W. C. Xu, H. L. Yuan, S. Gao, and Q. G. Crowley (2007b), A-type granite and adakitic magmatism association in Songpan-Garze fold belt, eastern Tibetan Plateau: Implication for lithospheric delamination, *Lithos*, *97*, 323–335.
- Zhang, X. K., S. X. Jia, J. R. Zhao, C. K. Zhang, J. Yang, F. Y. Wang, J. S. Zhang, B. F. Liu, G. W. Sun, and S. Z. Pan (2008), Crustal structures beneath west Qinling-east Kunlun orogen and its adjacent area: Results of wide-angle seismic reflection and refraction experiment [in Chinese with English abstract], *Chin. J. Geophys.*, *51*, 439–450.
- Zhang, Z. J., Y. H. Wang, Y. Chen, G. A. Houseman, X. B. Tian, E. C. Wang, and J. W. Teng (2009), Crustal structures across Longmen Shan fault belt from passive source seismic profiling, *Geophys. Res. Lett.*, *36*, L17310, doi:10.1029/2009GL039580.
- Zhang, Z. J., X. H. Yuan, Y. Chen, X. B. Tian, R. Kind, X. Q. Li, and J. W. Teng (2010), Seismic signature of the collision between the east Tibetan escape flow and the Sichuan Basin, *Earth Planet. Sci. Lett.*, *292*, 254–264.
- Zhao, Y. J., C. Yuan, M. F. Zhou, D. P. Yan, X. P. Long, and J. L. Li (2007), Geochemistry and petrogenesis of Laojungou and Mengtonggou granites in western Sichuan: Constraints on the nature of Songpan-Ganzi basement [in Chinese with English abstract], *Acta Petrol. Sin.*, *23*, 995–1006.
- Zhou, D., and S. A. Graham (1996), Songpan-Ganzi Triassic flysch complex of the West Qinling Shan as a remnant ocean basin, in *The Tectonic Evolution of Asia*, edited by A. Yin and M. Harrison, pp. 281–299, Cambridge Univ. Press, Cambridge, U. K.